

**Magnetoresistance analysis
of two-dimensional hole gases
in GaN/AlGaN/GaN double heterostructures**

S. Yamada^{1*}, A. Fujimoto¹, S. Yagi², H. Narui², E. Yamaguchi³
and Y. Imanaka⁴

¹*Osaka Institute of Technology,
5-16-1 Ohmiya, Asahi-ku, Osaka, 535-8585 Japan*

²*Powdec,
1-23-15 Wakagi-cho, Oyama-shi, Tochigi, 323-0028 Japan*

³*Kyoto University,
Yoshida-honmachi, Sakyo-ku, Kyoto, 606-8501 Japan*

⁴*National Institute of Materials Science,
3-13 Sakura, Tsukuba, Ibaragi, 305-0003 Japan*

Abstract

Magnetoresistance (MR) of 2D hole gas (2DHG) samples fabricated from GaN/Al_xGa_{1-x}N/GaN (x = 0.2~0.25) double heterostructures has been investigated to reveal subband electronic parameters and low field spin splitting properties. In sample with high sheet hole density ($p_s \leq 1.3 \times 10^{13} / \text{cm}^2$) 2DHG occupies two subbands, while in samples with low $p_s (\leq 0.3 \times 10^{13} / \text{cm}^2)$ only one subband is occupied. In both samples, the low-field spin-orbit coupling constant α of 2DHG were obtained independently from the weak anti-localization (WAL) data and the FFT analysis of MR oscillations. The results yield a constant $\alpha \sim 0.53 - 6.1 \times 10^{-12}$ eVm and a spin splitting $\Delta E = 2\alpha k_f \sim 0.6 - 6.0$ meV. These results strongly depend on the hole mass value, but appear to be of the same order as the results for 2D electron gas (2DEG) in similar material systems and structures.

*Corresponding author: shojiyamada038@outlook.com

Alongside silicon carbide (SiC), gallium nitride (GaN) is expected to be a next-generation power semiconductor material [e.g. 1-3]. This material has a high electron mobility, which makes it suitable for high-frequency applications requiring fast switching. In addition, the power losses generated during switching are small, resulting in low heat generation. On the other hand, for applications requiring high voltages and currents, SiC is currently the material of choice, as GaN devices are considerably more expensive. For this reason, SiC is mainly used in high-voltage applications, while GaN is expected to be used mainly in high-frequency applications.

In lateral GaN devices, current is conducted usually by a dense two-dimensional electron gas (2DEG) formed at the AlGaIn/GaN interface mainly due to the piezoelectric effect. Indeed, 2DEG samples with sheet electron density, $n_s \gg 1 \times 10^{13} / \text{cm}^2$ and mobility, $\mu \gg \sim 10^4 \text{ cm}^2/\text{Vsec}$ have been reported [e.g. 4], and their device applications have been extensively studied over the past 30 years. In this paper, however, we rather focus on the fundamental side, that is, subband transport physics including (low-field) spin properties of the 2DEGs, which has been carried out in parallel to the extensive application studies. For example, low-temperature magnetoresistance (MR) measurements have shown that 2DEGs with $n_s > 7 \times 10^{12} / \text{cm}^2$ occupy up to the first excited (second) subband [5]. Further refined MR measurements and analysis of weakly anti-localized (WAL) signals and beat vibration in Shubnikov de Haas (SdH) oscillations have revealed various low-field spin splitting properties that are important for future spintronic applications [e.g. 4, 6 and references therein]. Indeed, values of $0.6 - 7.85 \times 10^{-12} \text{ eVm}$ for the spin-orbit coupling constant α and $0.22 - 12.75 \text{ meV}$ for the low-field spin splitting $\Delta E = 2\alpha k_f$ have been reported (k_f is the Fermi wave vector, $(2\pi n_s)^{1/2}$); Note that α includes both α_{WAL} and α (beat), estimated respectively from WAL and beating measurements. We now briefly comment on the approximately one order of magnitude difference among α s in the tables in references 4 and 6, in terms of sub-band occupancy and difference in analysis methods. As mentioned above, when n_s is larger than the reference value ($\sim 7 \times 10^{12} / \text{cm}^2$), the ground and first excitation subbands are often occupied. In such cases (where n_s is relatively large), α (beat) is likely to be overestimated due to magnetic inter-subband scattering (MIS) [7]. Furthermore, WAL is generally known to give smaller spin splitting than that estimated by the beat method (even in narrow-gap semiconductor heterojunctions), although the reason for this is not yet clear.

On the other hand, research on two-dimensional hole gases (2DHGs) has rather progressed in the last two decades in terms of crystal growth and device fabrication. Indeed, GaN/AlGaIn single heterostructures, p-channel heterostructures [8-13] and GaN/AlGaIn/GaN double heterostructures (2DHG-2DEG coexistence systems) have been grown and studied. And based on these technologies, various 2DHG based p-channel FETs [14-19] and so-called polarized junction (PJ) FETs [20, 21] have been proposed, fabricated and studied. In recent years, the high-frequency and high-power performance of these devices has been significantly improved [22-25].

However, the fundamental transport (subband) physics of 2DHGs is still largely unresolved. Indeed, other than the work by S. J. Bader et al [26], there are few reports on subband and spin-related transport in GaN 2DHGs at low magnetic fields. This is probably due to the fact that, despite recent improvements in the quality of GaN/AlGaN 2DHGs (increased density and mobility) [24, 25], the relevant transport techniques are not sufficiently advanced for detailed fundamental studies. One of the difficulties in this type of technology is incomplete ohmic contact [27] to 2DHG. In addition, the effective mass values of 2DHG are not yet well known experimentally. However, for holes in wurtzite-type GaN, the masses of heavy and light holes at the band edge have been estimated by photoelectron spectroscopy studies [28] and the masses of heavy and light holes in the singular 2D plane have been discussed by phonon studies and calculations [26].

In this paper, low-temperature MR measurements of two 2DHG samples (5 mm square van der Pauw type with high and low sheet hole densities, p_s , sample P and H, respectively) fabricated in GaN/Al_xGa_{1-x}N/GaN ($x = 0.2\sim 0.25$) double heterostructure were performed. Electrodes were fabricated with NiAu, which can only contact to 2DHG. Two types of resistance measurements, low-field WAL and high-field MR, were performed and the signals were analyzed precisely. As a result, the electronic subband structure and the low-field spin state of 2DHG could be estimated: Two and one subband were found to be occupied in sample P with high $p_s \leq 1.3 \times 10^{13}/\text{cm}^2$ and in sample H with low $p_s \leq 0.32 \times 10^{13}/\text{cm}^2$, respectively. Typical spin-orbit coupling constant α and low-field spin splitting ΔE were found to be about $0.53 - 6.1 \times 10^{-12}$ eV m and $-0.6 - 6.0$ meV, respectively. Again, α includes both α_{WAL} and $\alpha(\text{beat})$. These results were discussed by comparing the values obtained for 2DEGs in the same GaN/AlGaN/GaN double heterostructure and narrow gap system ($\text{In}_{0.75}\text{Ga}_{0.25}\text{As}/\text{In}_{0.75}\text{Al}_{0.25}\text{As}$). For the measurement and analysis of WAL and MR data, we referred to a number of experiences [29-32] in low-quality, high contact resistance, multi-subband occupied heterojunction samples. Details on sample preparation/measurement and hole effective masses are given in the Supplementary Material.

In Fig. 1, we show the two-terminal (2t) and four-terminal (4t) WAL signals for sample H with a low n_s in the upper and lower panels, respectively. Perhaps due to the high contact resistances of the electrodes at low temperatures, the 2t and 4t WAL signals have a poor signal-to-noise (S/N) ratio and hence the WAL features were sometimes screened by the noise as seen in the figure. However, the WAL signal of the quality shown here was reproducibly confirmed for both 2t and 4t conductance, and the field B_{min} (green dashed eye-guides), where the conductance difference $\sigma(B) - \sigma(0)$ takes a minimum value, was almost identical for the two signals. Therefore, B_{min} was estimated to be $\sim \pm 40$ mT. The measurement of sample P with a high n_s was even easier due to the higher background conductance (low resistance) and B_{min} was almost the same as above. In the final stage, similar WAL signals with minima at $B_{\text{min}} \sim \pm 40$ mT were also identified in eight different samples and in samples

experiencing thermal histories between low temperature and room temperature. Furthermore, we have already successfully observed such WAL with similar noise levels in semiconductor samples of different semiconductor materials (narrow gap) [31].

The usual approach to estimating α for samples in the diffusive regime is to fit the WAL signal with a curve based on the so-called ILP theory [33]. Here, however, a simpler approximation involving this minimal field is adopted, as the accuracy of the curve fitting may be compromised due to the insufficient S/N ratio of the signal. From theory, the value of the spin-orbit coupling constant, $\alpha_{WAL} \sim \sqrt{e\hbar^3 B_{min}} / m^*$ [34], in the WAL case can be derived by substituting B_{min} : at $B_{min} \sim 40$ mT, assuming a heavy hole mass of 1.2 (0.4) m_0 , α_{WAL} is 0.53 (1.6) $\times 10^{-12}$ eVm and $\Delta E = 2\alpha_{WAL} k_f$ is found to be $0.5 - 0.6$ ($1.4 - 1.8$) meV.

Figure 2(a) shows the raw MR data of sample P up to 15 Tesla. Red and blue traces are the up-sweep and down-sweep signals, respectively and they are slightly offset with each other. At first glance it appears that both signals are only gradually monotonically increasing by $\sim 2\%$ at magnetic field $B = 0-15$ T. However, careful observation of the signals reveals very small oscillations that are similarly reproduced in the up- and down-sweep traces. Figure 2(b) shows the differential (dR_{xx} / dB) of the overall MR data for sample H as a function of B^{-1} (T^{-1}) in order to examine the signal in detail. Again, it can be seen that the red and blue traces correspond to up- and down-sweeps and are reproduced almost overlapping in the main field range ($0.1 - 0.7 T^{-1}$, i.e. $\sim 1.4 - 10$ T).

This result suggests that these signals may be significant signals rather than noise, and that analysis from a quantum mechanical point of view (Landau subbands) should be attempted. Indeed, in another experiment (not shown), where the direction of the magnetic field B was tilted from the surface normal of the sample, the main features of the oscillations were found to vary with the cosine law, supporting the two-dimensional nature of the signal. To obtain further evidence that the signal was a 2DHG SdH vibration, a careful Fast Fourier Transform (FFT) analysis was performed on the SdH data including the derivatives. n_s values were then obtained from the FFT spectrum and compared with the Hall measurement results (see Supplement).

The upper and lower panels of Figure 3 show the FFT results of the first derivative dR_{xx} / dB of the MR data obtained for samples P and H, respectively. For a simple and direct understanding of the spectra, we start the analysis and discussion with the lower panel corresponding to the simpler case, sample H. Sample H has a small p_s , so the 2DHG is expected to occupy only the one (ground) subband; if we consider the major peak (indicating a split) in $B_c < 100$ T corresponds to an occupied subband, the p_s s corresponding to the two split peaks (indicated by the green dashed eye guide) are 0.1 and $0.15 \times 10^{13} / \text{cm}^2$ from the equation $(e/h) B_{c,peak}$ for the non-degenerate case. Summing these, the total p_s of the subband is estimated to be $(2e/h) B_{c,peak} \sim 0.25 \times 10^{13} / \text{cm}^2$. The position of $B_{c,peak} \sim 52$ T

corresponding to the sum (average) of the two split peaks is indicated by the green triangle on the far left. This p_s value has an error of about 20% with the Hall measurement result of $0.32 \times 10^{13} / \text{cm}^2$. The higher $B_{c \text{ FFT}}$ peaks (similarly indicated by the solid green triangle but without splitting) are probably harmonics of the main peak on the far left.

However, in the upper panel of sample P, there are two large peaks at $B_c < 150$ T, each with a peak separation (blue dashed guides). These two large peaks can be interpreted without problems if we assume that the heavy holes (or heavy and light holes) occupy the ground and first excited subbands (respectively) of sample P. Analyzing each peak in the same way as for sample H above, assuming that the two subbands are occupied, the sample P also gives a p_s value of $(0.18+0.22)$ (low major peak) + $(0.27+0.33)$ (high major peak) $\sim 1.0 \times 10^{13} / \text{cm}^2$. This value is also about 20% lower than the Hall measurement ($1.3 \times 10^{13} / \text{cm}^2$); the $B_c > 150$ T peak is likewise considered to be part of the harmonics of the two major peaks: some peaks and harmonics are indicated by solid and open blue triangles (corresponding to the lower major and upper major peaks, respectively), but their origin is not entirely clear due to the complexity of the FFT results.

Thus, the estimated p_s values of the main peaks in the FFT data analysis of samples H and P were found to be $\sim 20\%$ smaller than the Hall measurements. The reason for this discrepancy is probably the three-dimensional (3D) Hall conduction. Excluding this effect and taking into account the general error of the Hall measurements ($\sim 10\%$), the p_s results of the MR and Hall measurements are considered to be in good agreement. This result strongly suggests that the small oscillations observed in MR (R_{xx}) are due to SdH oscillations reflecting the interfacial 2D electronic structure of 2DHG. As is well known, in a normal 2D carrier system, the sheet carrier density is proportional to the energy subband level (difference) by the formula $E_f - E_i = \pi \hbar^2 p_s / m^*$, where E_i is the bottom level of the i -th 2D subband. Using the above equation to estimate the energy difference between the two 2D subbands of sample P, we obtain $E_f - E_i \sim 7.9$ (~ 24) and ~ 12 (~ 36) meV for the shallow ($p_s \sim 0.4 \times 10^{13} / \text{cm}^2$) and deep ($0.6 \times 10^{13} / \text{cm}^2$) subbands, respectively. The heavy hole mass m^* assumed here is 1.2 (0.4) m_0 . See Supplementary Material for a detailed discussion on hole masses.

In order to determine the normalized wavefunction and E_i of the relevant hole subbands, so-called self-consistent calculations might be useful. However, such calculations are not performed here. One reason is that the computational model for highly piezoresistive GaN heterojunctions is not established yet and there are many unknown parameters. Another is that, although subjective manipulation of parameters can yield plausible results that mimic the sample, there is no guarantee that the results reflect the sample quantitatively. Instead, from the peak separation of the major peaks, the key information α and $\Delta E = 2\alpha k_F$ evaluated earlier in the WAL analysis, can be estimated in a different way. The peak separation gives the beating parameter, $(\Delta i / \Delta(B^{-1}))$ (T) and α is estimated via the equation, $\alpha(\text{beat}) \approx \left(\frac{e\hbar}{2m^* k_F} \right) (\Delta i / \Delta(B^{-1}))$ [35]. The values of α obtained for samples P and H by

this method were α (*beat*) $\sim 2.0 - 2.1$ ($6.0 - 6.2$) $\times 10^{-12}$ eVm assuming $m_{\text{HH}}^*/m_0 = 1.2$ (0.4).

The electronic subband structures and spin-related parameters of 2DHGs in GaN/AlGaIn/GaN heterostructures estimated in this paper are summarized in Table 1. For comparison, 2DEG results obtained in narrow-gap In_{0.75}Ga_{0.25}As/In_{0.75}Al_{0.25}As [36] and in GaN/AlGaIn/GaN heterojunctions are also given. The effective masses used in the calculations are from the literature [37, 26, 28]. The GaN/AlGaIn/GaN 2DEG van der Pauw sample (sample E) is a rectangular cut from a wafer with the same layer structure as sample P(H), with Ti/Al/Ni/Au alloy as ohmic contact to the 2DEG.

The first important result is that the p_s values obtained from the SdH analysis are approximately equal to those obtained from the Hall measurements with an error of about 20%, as described above. The second result of note is that for the spin properties at low fields, the spin-orbit coupling constant α and the spin splitting ΔE were estimated from both MR WAL and beat FFT analyses. For the former, $\alpha_{\text{WAL}} \sim 0.53$ (1.6) $\times 10^{-12}$ eVm was obtained for both the samples P and H assuming $m_{\text{HH}}^*/m_0 = 1.2$ (0.4). On the other hand, α (*beat*) is found to be ~ 2.0 (6.1) $\times 10^{-12}$ eVm, which is about four times larger than α_{WAL} . The spin splitting corresponding to α_{WAL} and α (*beat*) is $\Delta E \sim 0.6 - 2.2$ ($\sim 2.0 - 6.0$) meV for the 2DHG samples. These values are close to or on the same order of magnitude as the 2DEG values estimated for sample E and reported in various previous GaN/AlGaIn 2DEG papers [4, 6].

Ultimately, in terms of the magnitude of the spin splitting, the 2DHG of the GaN/AlGaIn heterojunction system is almost similar to the properties obtained from a 2DEG with the same material structure. By studying the gate voltage dependence of the WAL signal, it will be possible to conclude which Rashba effect in the bulk [38] or at the interface [39, 40] is responsible for this splitting. Indeed, in the case of 2DEGs in GaN/AlGaIn heterojunctions [41], the WAL signal is very robust to gate voltage, i.e. n_s change, leading to the conclusion that the bulk Rashba effect is appropriate.

The magnetoresistance of 2DHG samples fabricated from GaN/AlGaIn/GaN double heterostructures has been investigated, revealing their subband structure and low-field spin splitting properties. In the high- p_s ($\leq 1.3 \times 10^{13}$ /cm²) sample P, the 2DHG occupies two subbands (base and first excitation) in the form of heavy and light holes or both heavy holes, whereas in the low- p_s ($\leq 0.32 \times 10^{13}$ /cm²) sample H, heavy hole one subband occupation seems to be found. In both samples, reproducible WAL signals and small MR oscillations with splitting of the main peak in their FFT spectra were observed. From these analyses, p_s values from Hall and MR analysis were in good agreement. Moreover, by assuming $m_{\text{HH}}^*/m_0 = 1.2$ (0.4), the spin-orbit coupling constant $\alpha \sim 0.53 - 2.0$ ($1.6 - 6.1$) $\times 10^{-12}$ eVm and the spin splitting $\Delta E = 2\alpha k_f \sim 0.6 - 2.2$ ($2.0 - 6.0$) meV were evaluated. These were found to be similar to those of GaN/AlGaIn 2DEGs. This low-field spin splitting probably originates from the Rashba effect due to the bulk crystal or interface piezoelectric field. In spin device applications, sensitivity to gate voltage is more important than the absolute values of α and ΔE . To elucidate the origin of spin splitting and to develop GaN/AlGaIn 2DHG spin devices, samples with

gate electrodes should be studied in the near future.

Supplementary Material

We give a short explanation with two figures about sample preparation and measurement. About hole masses of GaN also, a brief discussion is given with tables of possible mass values.

We sincerely acknowledge the support of JSPS Grant-in-Aid for Scientific Research 20K04631. We also thank Prof Takuma Tsuchiya and Prof Takaaki Koga of Hokkaido University for valuable discussions throughout this work.

References

- [1] X. L. Wang, T. S. Cheng, Z. Y. Ma, G. X. Hu, H. L. Xiao, J. X. Ran, C. M. Wang, W. J. Luo, *Solid State Electronics*, 51, 428 (2007).
- [2] Z. Chen, Y. Pei, S. Newman, R. Chu, D. Brown, R. Chung, S. Keller, S. P. Denbaars, S. Nakamura and U. K. Mishra, *Appl. Phys. Lett.*, 94, 112108 (2009).
- [3] N. Xu, R. Hao, Fu Chen, X. Zhang, P. Zhang, X. Ding, L. Song, G. Yu, Kai Cheng, Y. Cai, and B. Zhang, *Appl. Phys. Lett.*, 113, 152104 (2018).
- [4] S. B. Kisesivdin, N. Balkan, O. Makarovskiy, A. Patane, A. Yildiz, M. D. Caliskan, M. Kasap, S. Ozececik and E. Ozbay, *Appl/ Phys. Lett.*, 105, 093701 (2009).
- [5] Z. W. Zheng, B. Shen, R. Zhang, Y. S. Gui, C. P. Jiang, Z. X. Ma, G. Z. Zheng, S. L. Guo, Y. Shi, P. Han, Y. D. Zheng, T. Someya and Y. Arakawa, *Phys. Rev. B* 62, R7739 (2000); M. Sumiya, D. Kindole, K. Fukuda, S. Yashiro, K. Takehana, and Y. Imanaka, *Phys. Stat. Sol. B*, 257, 1900524 (2020).
- [6] I. Lo, M. H. Gau, J. K. Tsai, Y. L. Chen, Z. J. Chang, W. T. Wang, J. C. Chiang, T. Aggerstam, and S. Lourduoss *Phys. Rev. B* 75, 245307 (2007).
- [7] Z. J. Qiu, Y. S. Gui, T. Lin, N. Dai, J. H. Chu, N. Tang, J. Lu and H. Shen, *Phys. Rev. B* 69, 125335 (2004).
- [8] M. S. Shur, A. D. Bykhovski, R. Gaska, J. W. Yang, G. Simin, and M. A. Kahn, *Appl. Phys. Lett.*, 76, 3061 (2000).
- [9] M. Shatalov, G. Simin, J. Zhang, V. Adivarahan, A. Koudymov, R. Pachipulusu, and M. A. Khan, *IEEE Electron Device Lett.*, 23, 452 (2002).
- [10] T. Zimmermann, M. Neuburger, M. Kunze, I. Daumiller, A. Denisenko, A. Dadgar, A. Krost, and E. Kohn, *IEEE Electron Device Lett.* 25, 450 (2004).
- [11] M. Fandrich, T. Mehrrens, T. Aschenbrenner, T. Klein, M. Gabbe, S. Figge, C. Kruse, A. Rosenauer, and D. Hommel, *J. Crystal Growth*, 370, 68 (2013).
- [12] G. Li, R. Wang, B. Song, J. Verma, Y. Cao, S. Ganguly, A. Verma, J. Guo, and H. G. Xing, *IEEE Electron Device Lett.*, 34, 852 (2013).
- [13] F. Chen, R. Hao, C. Yu, X. Zhang, L. Song, J. Wang, Y. Cai and B. Zhang, *Appl. Phys. Lett.*, 115, 112103 (2019).
- [14] A. Scar, S. B. Liesesivdin, M. Kasap, S. Ozececik, and E. Ozbay, *Thin Solid Films* 516, 2041 (2008).
- [15] C. Buchheim, R. Goldhahn, G. Gobsch, K. Tonisch, V. Climia, and F. Niebelschutz, and O. Ambacher, *Appl. Phys. Lett.*, 92, 013510 (2008).
- [16] A. Nakajima, Y. Sumida, M. H. Dhyani, H. Kawai, and E. M. Sankara Narayanan, *Appl. Phys. Exp.* 3, 121004 (2010).
- [17] H. Hahn, B. Reuters, A. Pooth, B. Hollander, M. Henken, H. Kalisch, and A. Vescan, *IEEE*

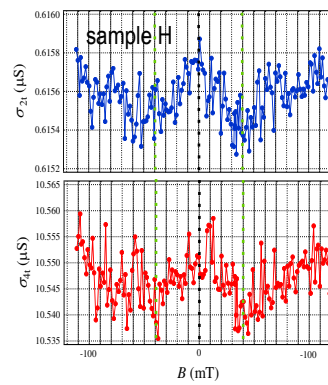
- Transactions Electron Devices, 60, 3005 (2013).
- [18] C. A. Hurni, J. R. Lang, P.G. Burke, and J. S. Speck, , Appl. Phys. Lett., 101, 102106 (2012).
- [19] H. Hahn, B. Reuters, S. Geipel, M. Schauerte, F. Benkhelifa, O. Ambacher, H. Kalisch, and A. Vescan, J. Appl. Phys., 117, 104508 (2015).
- [20] A. Nakajima, K. Adachi, M. Shimizu and H. Okumura, Appl. Phys. Lett. 89, 193501 (2006).
- [21] H. Kawai, S. Yagi, S. Hirata, F. Nakamura, T. Saito, Y. Kamiyama, M. Yamamoto, H. Amano, V. Unni, and E. M. S. Narayanan, Phys. Status Solidi A, 1600834 (2017).
- [22] R. Chaudhuri, R. S. J. Bader, Z. Chen, D. A. Muller, H. G. Xing, D. Jena, Science 365, 1454 (2019).
- [23] N. Chowdhury, J. Lemettinen, Q. Xie, Y. Zhang, N. S. Rajput, P. Xiang, K. Cheng, S. Suihkonen, H. W. Then, T. Palacios, IEEE Electron Device Lett., 40, 1036 (2019).
- [24] N. Chowdhury, Q. Xie, M. Yuan, N. S. Rajput, P. Xiang, Ka. Cheng, H. W. Then, and T. Palacios, 2019 IEEE International Electron Devices Meeting (IEDM), pp. 4.6.1-4.6.4.
- [25] K. Nomoto, R. Chaudhuri, S. J. Bader, L. Li, A. Hickman, S. Huang, H. Lee, T. Maeda, H. W. Then, M. Radosavljevic, P. Fischer, A. Molnar, J. C. M. Hwang, H. G. Xing, D. Jena, 2020 IEEE International Electron Devices Meeting (IEDM), pp. 8.3.1-8.3.4.
- [26] S. J. Bader, R. Chaudhuri, M. F. Schubert, H. W. Then, H. G. Xing, D. Jena, Appl. Phys. Lett., 114, 253501 (2019).
- [27] F. G. Kalaitzakis, N. T. Pelekanos, P. Prystawko, M. Leszczynski, and G. Konstantinidis, Appl. Phys. Lett., 91, 261103 (2007).
- [28] M. Franz, S. Appelfeller, H. Eisele, P. Ebert, and M. Dahne, Phys. Rev. B99, 195306 (2019).
- [29] S. Yamada and T. Makimoto, Appl. Phys. Lett., 57, 1022 (1990).
- [30] K. Maezawa, T. Mizutani and S. Yamada, J. Appl. Phys., 71, 296 (1992).
- [31] M. Akabori, S. Hidaka, H. Iwase, S. Yamada and U. Ekenberg, J. Appl. Phys. 112, 113711 (2012).
- [32] S. Yamada, A. Fujimoto, S. Hidaka, M. Akabori, Y. Imanaka, and K. Takehana, Sci. Rep., 9, 7446 (2019).
- [33] S. V. Iordanskii, Y. B. Lianda-Gellar, G. E. Pikus, JETP Lett., 60, 206 (1994).
- [34] S. Faniel, T. Matsuura, S. Mineshige, Y. Sekine and T. Koga, Phys. Rev. B83, 115309 (2011).
- [35] Th. Schapers, G. Engels, J. Lange, Th. Klocke, M. Hoffelder, and H. Luth, J. Appl. Phys., 83, 4324 (1998).
- [36] Private communication. Recent typical result in our group.
- [37] T. Y. Lin, H. M. Chen, M. S. Tsai, Y. F. Chen, F. F. Fang, C. F. Lin and G. C. Chi, Phys. Rev B58, 13793 (1998).
- [38] E. I. Rashba and V. I. Sheka, Symmetry of energy bands in crystals of wurtzite type: II. Symmetry of bands including spin-orbit interaction *Fiz. Tverd. Tela: Collected Papers* 2 162–76 (1959). English translation is given as the supplementary material to the article by Bihlmayer et al, New. J. Phys. 17

050202 (2015).

[39] F. J. Ohkawa and Y. Uemura, *J. Phys. Soc. Jpn.* 37 1325–33 (1974).

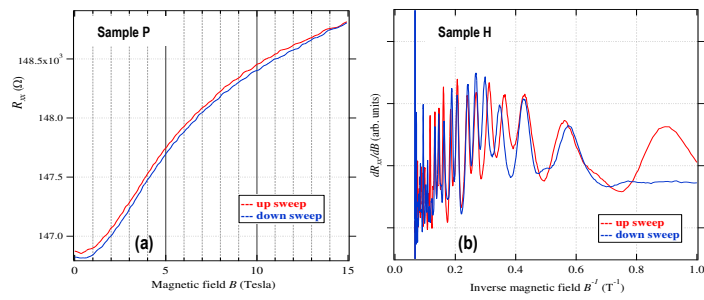
[40] Y. Bychkov and E. I. Rashba, *J. Phys. C* 17, 6039 (1984).

[41] N. Thillosen, S. Cabanas, N. Kaluza, V. A. Guzenko, H. Hartdegen, and Th. Schapers, *Phys. Rev. B* 73, 241311(R) (2006).



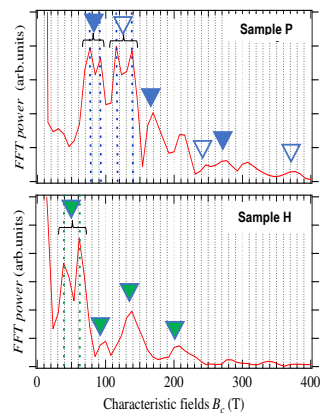
S. Yamada Figure 1

Fig. 1 Typical WAL signal for sample H with relatively high (electrode) contact resistance at low temperature: the upper and lower traces correspond to the two-terminal conductance σ_{2t} and four-terminal conductance σ_{4t} , respectively. The black and green dashed lines indicate the position of the zero field ($B = 0$) and the minimum σ field (B_{min}), respectively. For cross-checking the minimum characteristics in positive and negative symmetrical magnetic fields, the two traces were measured and recorded simultaneously. As shown in the figure, the typical characteristics of the WAL signal are reproduced, although the signal-to-noise (S/N) ratio is not relatively high. Almost similar WAL signals could easily be observed in sample P due to its lower (contact) resistance than in sample H.



S. Yamada Figure 2(a) (left) and (b) (right)

Fig. 2 (a) Four-terminal longitudinal resistance R_{xx} of sample P. There is a slight shift (hysteresis) between the signals of the upward (red) and downward (blue) sweeps of the magnetic field. (b) dR_{xx}/dB signal of sample H. Due to the difference operation on the original R_{xx} , we can clearly confirm the fact that dR_{xx}/dB s are reproduced between the upward and downward field sweeps, especially in the main field range of $B^{-1} = -0.1 - 0.7 \text{ T}^{-1}$, i.e. $B = \sim 1.4 - 10 \text{ T}$, which in turn guarantees the reproduced behavior of R_{xx} itself against field sweep directions. These results strongly suggest that the very small oscillations superimposed on the R_{xx} background originate from magnetic quantum phenomena, i.e. Landau quantization of the 2DHG subband.



S. Yamada Figure 3

Fig. 3 FFT results of the signal dR_{xx}/dB_s obtained for sample P (top) and sample H (bottom). In the upper figure, there are two large peaks at low fields below 150 T (indicated by the solid and open triangles), both of which may correspond to the two subbands occupied by the 2DHG. There is also a peak split in each of them (probably due to spin separation), the position of which is indicated by the blue dashed lines. The peaks located at higher fields than them (shown by similarly solid or open blue triangles) are considered to be part of the second and third harmonics, which have no clear peak splitting. The bottom panel shows the results for sample H, which shows almost the same behavior as sample P (top panel), but with a simpler spectrum with only one subband occupied by the 2DHGs due to the smaller p_s . In other words, the spectrum consists of a main peak ($B_c \sim 50$ T, green solid triangle) with a split peak (green dashed line) and several associated harmonics (also green triangle). Thus, by estimating the origin of the main peaks and analyzing them in detail, information on the sheet hole density and spin splitting of each subband occupied by 2DHG can be obtained.

S. Yamada

Table 1 Summary of detailed subband electronic parameters and low-field spin properties of GaN/AlGaIn/GaN double heterojunction 2DHGs estimated in this study.

Material	In _{0.75} Ga _{0.25} As 2DEG	GaN 2DEG(E)	GaN 2DHG(P)	GaN 2DHG(H)
n_s/p_s ($\times 10^{13}/\text{cm}^2$) (Hall) { n_s/p_s ($\times 10^{13}/\text{cm}^2$) (FFT)}	0.064	0.78	1.3 {1.0 ~ (0.18+0.22) + (0.27+0.33)}	0.32 {0.25~ (0.10+0.15)}
μ (cm^2/Vsec) (Hall)	44,000	1,000	12	7
m^*/m_0	0.04	0.22	1.2 (0.4)	1.2 (0.4)
B_{min} (mT)	5	2	40	40
α_{WAL} ($\times 10^{-12}$ eVm)	5.1	0.63	0.53 (1.6)	0.53 (1.6)
$\Delta E_R = 2\alpha_{WAL}k_F$ (meV)	2.0	0.88	0.6 (1.8)	0.5 (1.4)
$\alpha(\text{beat})$ ($\times 10^{-12}$ eVm)	7.6	3.9	2.1 (6.2)	2.0 (6.0)

Note: For comparison, results obtained for 2DEGs in narrow-gap (In_{0.75}Ga_{0.25}As / In_{0.75}Al_{0.25}As) and in GaN/AlGaIn/GaN double heterojunctions are also given; the effective masses for 2DEG and 2DHG in GaN are the values from Refs [36, 26, 28]. Other parameters were measured or estimated values from measurements via appropriate equations described in the text: $\alpha_{WAL} \sim \sqrt{e\hbar^3 B_{min}} / m^*$ and $\alpha(\text{beat}) \approx \left(\frac{e\hbar}{2m^* k_F} \right) (\Delta i / \Delta(B^{-1}))$. k_F is a Fermi wave vector, $(2\pi n_s)^{1/2}$.